한국전산구조공학회
1994년도 가을학술발표회 논문집

조립식 지붕 외장 시스템에 대한 풍하중 평가
Wind Effects on Loose-Laid Roofing Paver Systems

함 희정[1] 이 재홍[2]
Hee-Jung Ham Jaehong Lee

Abstract

Full-scale and 1:15 scale fluid model experiments of roof ballast pavers are employed to optimize paver geometry and study wind loading and performance of roof ballast pavers. Wind pressures above and beneath pavers are conducted for buildings of different heights and in different flow conditions. The effects of the side hole size and the underneath rib height under the wind loading on pavers and the effects of roof parapet height as well as flow conditions on the performance of pavers are studied. Incorporation of wind tunnel experimental results into code statements is also provided.

1. Introduction

Typical industrial buildings have block type shapes with roofs which are flat or only marginally inclined. In recent years an idea of loose-laid roofing systems has been developed for such flat-topped buildings in northern America. The main components of these systems are ballasting pavers which are loose-laid on top of an impermeable membrane which covers the insulation and supporting systems of the roof. The pavers are placed on the whole roof or, when combined with gravel, placed in roof areas of high anticipated wind suction pressure, mainly near the roof corners and along the edges. Due to the negative wind suction acting on the exterior surface of roofs, such systems are prone to failure in strong winds through dislodging or overturning of pavers.

The performance of loose-laid roofing system is strongly affected net wind uplift acting on the ballasting elements and a roof membrane. The uplift is the net result of wind pressure exerted on the exterior and interior surfaces of ballasting elements. The distribution of wind pressure on the exterior surface of a roof is closely related to the characteristics of flow over the roof. Flow separates from the windward edge and corner regions of the roof and this results in a distinct flow pattern and pressure distribution. For typical building geometries it has been found that cornering winds create the highest pressure suctions. As a result, such winds and associated pressures are considered to be critical in studies and design of roofing systems.

In order to understand these phenomena and to provide reliable data for design, wind tunnel investigation was conducted by Ham et al.[1] in Colorado State University. The present paper summarizes new results obtained from the wind tunnel test. The experimental study consists of two main phases. First wind pressure is measured for a full-scale model of paver to determine the effects of hole size (at the vertical paver side) and effects of underneath rib height of the paver. Based on the measured external and underneath pressures, the net wind uplift acting on the paver is calculated for different hole sizes and

1) 현대건설 기술연구소 연구원
2) 현대건설 기술연구소 선임연구원

underneath rib heights. Next, the failure wind speed and the wind pressure measurements are carried out for a 1:15 geometrical scale model of the paver placed on the top of generic building model placed in three atmospheric boundary layer flows, Wind Exposure A, B and C of ANSI/ASCE-88. The mean failure wind speed for different roof parapet heights is acquired and the external and underneath pressure distributions for representative configurations are obtained. Incorporation of fluid model results into design provision, UBC and ANSI, is also presented.

2. Facilities and Experimental Configuration

2.1 Full-scale Wind Tunnel Test

The wind tunnel used for the full-scale paver model was Eiffel type wind tunnel which had 12ft wide, 7ft high and 57ft long working section. Fig. 1] shows plan and elevation views of the full-scale paver model. The size of opening is adjustable by changing the dimension denoted by w in Fig. 1]. This allows for testing the effects of the permeability of the paver. The details of the full-scale paver model are shown in Fig. 2]. Wooden strips are attached to the side surface along the longer paver edge. The length of the strips is varied to test the effects of the paver hole size on the pressure underneath the paver.

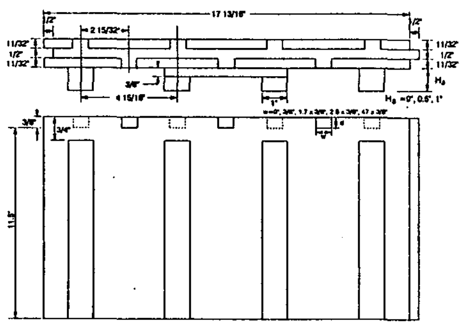

Fig. 1] Dimensions of Full-Scale Paver Model

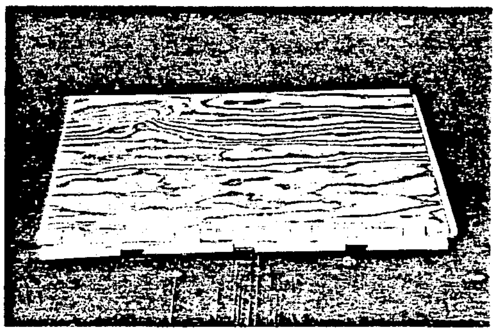

Fig. 2] Full-Scale Paver Model for Wind Tunnel Test

The model pavers in Fig. 2] are arranged in a staggered configuration on a platform assembled in the wind tunnel as shown in Fig. 3]. Since the purpose of the experiment is to test relative effects of paver permeability, large blockage ratio in the wind tunnel is not considered to be a critical factor. Fig. 4] depicts the pressure tap locations (solid circles) on the platform for the arrangement of the pavers.

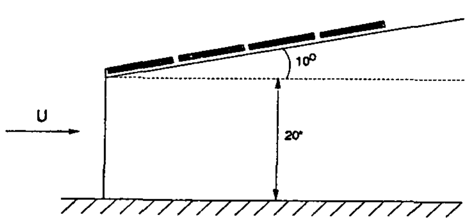

Fig. 3] Platform for Full-Scale Test

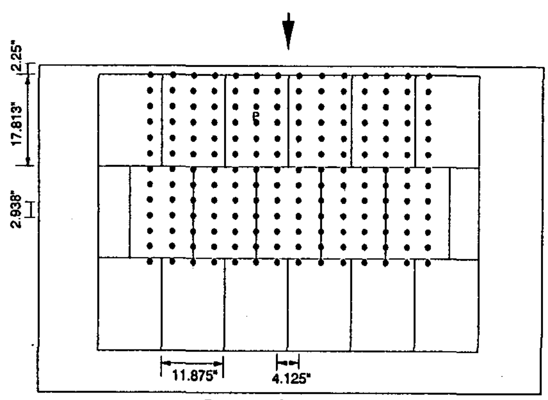

Fig. 4] Pressure Tap Location and Paver Configuration

2.2 1:15 Scale Wind Tunnel Test

The study of paver performance and the wind loading was conducted in Gottinggen type wind Tunnel. The wind tunnel has a test section of 6 ft wide and 6 ft high. Three simulated atmospheric boundary layer flows were used in the testing. Power law exponent for each Exposure is 0.28, 0.23 and 0.15, respectively

2.2.1 Similitude Requirements for Fluid Modeling of Roof Ballast Systems

Wind-tunnel model tests must satisfy certain similarity criteria in order to be representative of prototype conditions. This will be achieved if the wind approaching the model has the value for the main nondimensional flow parameters as the prototype flow. In the present study, the main flow parameters are represented by Reynolds number UL/ν, and Froude number U^2/Lg. The Reynolds number relates the relative ratio of inertial and viscous forces in the flow, whereas the Froude number relates the inertial lift forces of the air to the relative weight of the pavers. It is impossible to match both the Reynolds number and Froude numbers in a fluid model experiment. It is well established that flows over sharp edged objects are independent of Reynolds number for moderately high Reynolds number. As a result, the Reynolds number similarity requirement, Froude number, is satisfied when the wind speed scale λ_U and the geometrical scale λ_L are related as follows;

$$\lambda_V = \lambda_L^{1/2} = \left(\frac{L_m}{L_p}\right)^{1/2}. \quad (1)$$

This relation can be used to compute the prototype wind speed corresponding to a given wind-tunnel speed. The wind-induced motion of the paver model also must be dynamically similar to that of the prototype paver. This requires that the mass ratio (mass of air/mass of paver) must be the same for the model and for the prototype. In the case of thin objects such as insulation boards or pavers, Bienkiewicz[1] concluded that scaling of the density ratio can be relaxed and replaced by the similarity requirement that the weight per unit area ratios be the same for model and prototype, or as follows;

$$\frac{(\sigma t)_m}{(\sigma t)_p} = \frac{L_m}{L_p}, \quad (2)$$

where σ is paver density; t denotes paver thickness; and the subscripts m and p denote model and prototype, respectively.

2.2.2 Paver and Building Models

Based on the experimental results for the full-scale paver and similarity requirement for mass ratio, the 1:15 geometrical scale paver models are used in the wind tunnel experiments. The scaled paver model consists of three parts; main part, ribs and strips. The main part is made of plexiglass and represented the paver geometry without side holes as shown in Fig. 5].

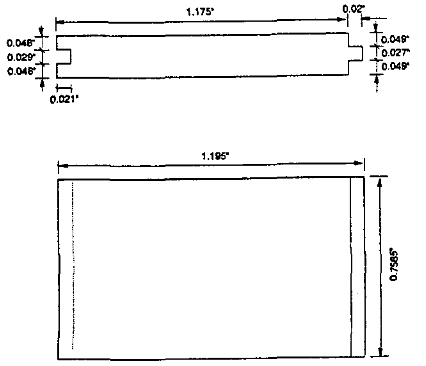

Fig. 5] Basic Dimensions of 1:15 Scale Paver Model

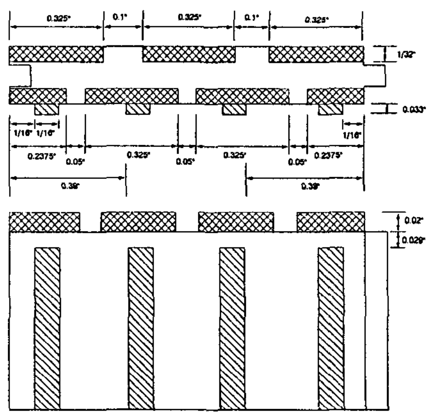
Fig. 6] Geometric Details of 1:15 Scale paver Model

Ribs and strips are represented using thick graphic tape as shown Fig. 6]. Due to the size of the model paver, the number of holes is reduced, however the hole size is increased to correctly model the permeability of the prototype paver.

For paver failure tests, the 1:15 scale paver model is put on the roof of a 1:15 scale generic building model. The dimensions of the building are described in Fig. 7], and the layout for paver system is shown Fig. 8].

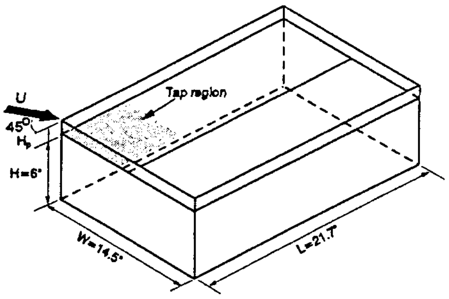

Fig. 7] Dimension of Building Model

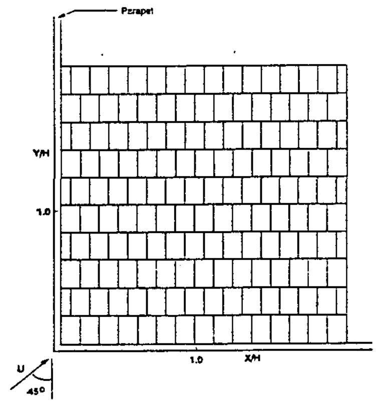

Fig. 8] Arrangement of 1:15 Scale Paver Model

3. Wind Tunnel Tests and Results

3.1 Optimization of Paver Geometry

The objective of the experiments described in this section is to find the configuration of the paver with the best wind resistant properties. This is achieved through the investigation of the effects of side holes and bottom ribs on the paver under the wind loading. Since the wind net uplift on a paver is the difference between the underneath pressure and the external pressure, and the external pressure does not depend on paver geometry[2], only the effects of paver geometry on the underneath pressure need to be considered. The higher (in magnitude) the underneath suction, the more wind-resistant is the paver.

Wind pressure distribution above and beneath the full-scale paver model was measured for different paver configurations. For each configuration, underneath mean and negative peak pressure distributions were measured and the differences between the underneath and external mean and negative peak pressures were calculated. The pressure distribution on the exterior surface, measured on a bare roof is shown in Fig.9]. As can be seen in Fig. 9], high negative pressure occurs in the region close to the windward roof edge, while high pressure gradient appears further down stream. The tested combinations of w and H_s are shown in Table 1]. In the table, w/d = 0 corresponds to the case when there is no opening, whereas w/d = 47 corresponds to the case when there is no strips between the pavers and the space between pavers is totally open.

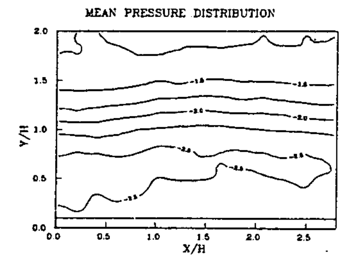

Fig 9] External Pressure Distribution on the Full-Scale Model

Table 1] Tested Paver Hole and Rib Dimensions (w and H_s)

Hs \ w/d*	0.0	1.0	1.7	2.5	47.0
0.0"	O	O	O	O	O
0.5"	O	O	O	O	O
1.0"	O	O	O	O	O

d* = 3/8" and "O" indicates the combination

Uplift distributions for different hole sizes and rib heights are shown in Fig. 10]. In case Hs =1 and w/s = 0, higher positive uplift (pressure difference) can be seen. This suggests that pavers in this region may fail if wind is strong enough. As w/d increases the level of 47, this positive uplift disappears. Thus, in turn, indicates that large hole size make paver more wind-resistant. Reducing rib height also removes positive uplift at the roof edge area.

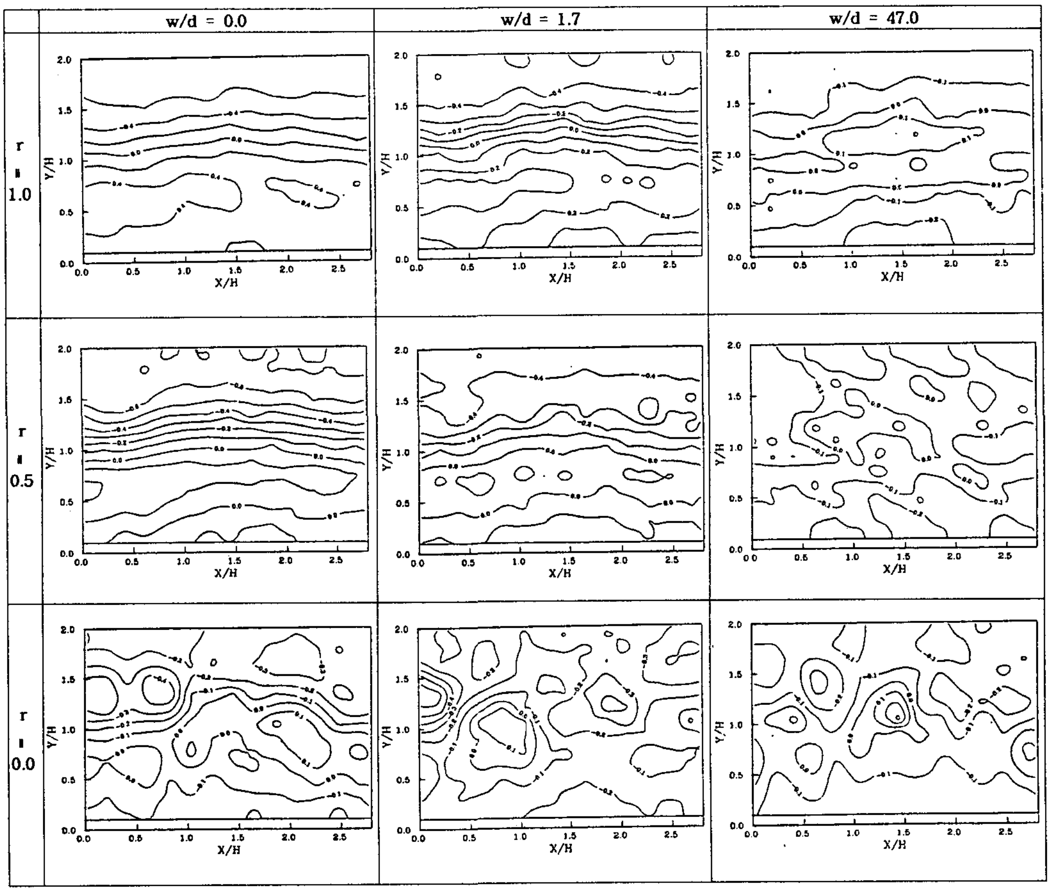

Fig. 10] Difference of Underneath and External Mean Pressure

The effects of hole size and rib height on the underneath pressure of pavers are shown in Fig. 11] with overall maximum underneath mean and peak pressure for different hole and rib height.

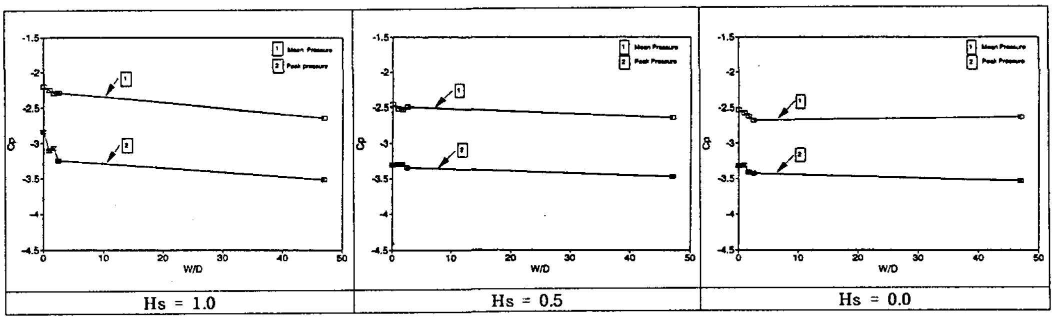

Fig. 11] Overall Maximum Underneath Mean and Peak Pressure

Because uplift is difference between external pressure and underneath pressure, high underneath pressure makes paver more wind-resistant. It can be seen that the increase in hole size slightly increases the magnitude of the underneath pressure. Reduction in the underneath rib height also results in higher magnitude of the underneath pressure. As a result, the spacing between pavers had beneficial effects while the spacing beneath pavers had detrimental effects on the wind resistance of the pavers.

4.2 Failure Wind Speed

Fig. 12] depicts the failure wind speeds at different roof parapet heights for the building in flow A, B and C, respectively. In the figures, the failure wind speed is converted to the full-scale wind speed (miles-per-hour), and the parapet H_P is normalized by the building height, H. It can be found from these figures that very low roof parapet slightly reduces the failure wind speed, making the paver system less wind-resistant. However, for higher parapets, the failure wind speed significantly increases. Comparing the failure wind speed for the same roof parapet height of the building in different flows, it can be seen that in flow A the failure wind speed is the lowest and in flow C it is the highest, with values for flow B falling in between. This is because flow A has much higher turbulence level at roof height than flow B and C.

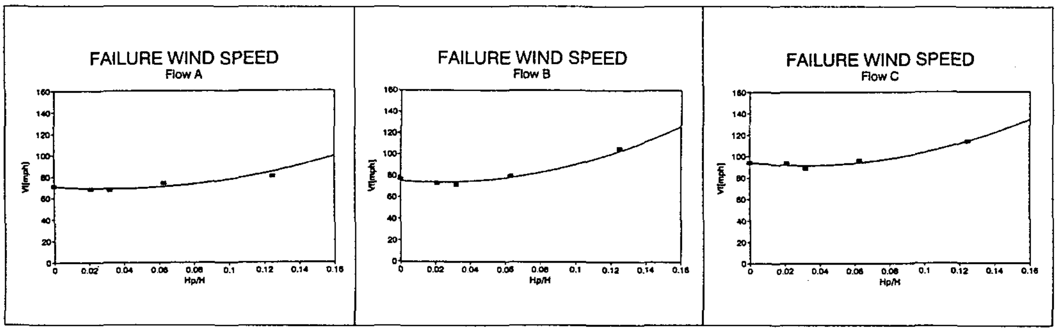

Fig 12] Comparison of Flow Effects on Failure wind Speed

Fig. 13] shows representative failure patterns of this loose-laid roof system. The shaded pavers were those which failed, i.e., were dislodged by wind. The paver marked "★" is the one that failed first. In general, pavers close to the windward roof corner edge (X axis) failed first. Ham[3] shows the relationships between paver failure and pressure distribution in this area.

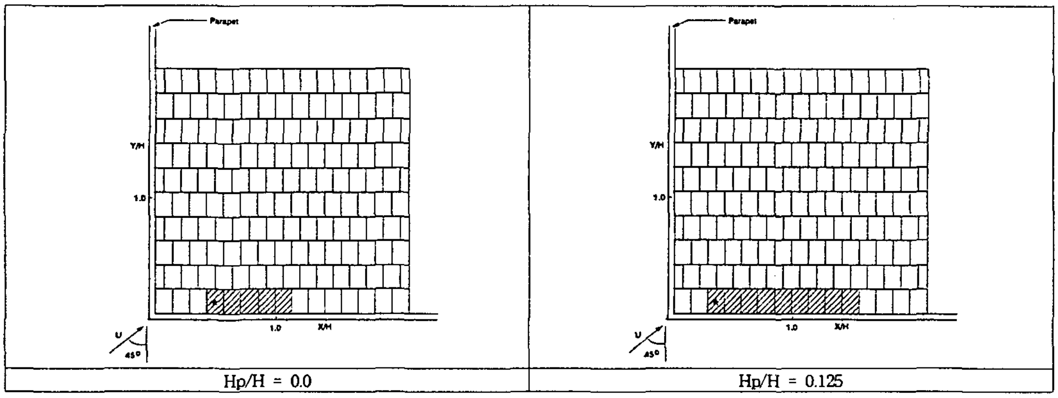

Fig 13] Failure Patterns of Roof Pavers in Flow A

5. Design considerations

The design approach developed by Bienkiewicz and Meroney[4] is slightly modified and applied in the present study. The approach is based on the *minimum failure wind speed* determined experimentally for a given paver configuration, building height and flow condition.

The failure wind speed V_F has been defined as the mean wind speed at the building roof heights at which the paver failure occurs. The design, or basic wind speed V, is specified by codes and standards as the speed at a height of 10 m. The peak wind speed at the building roof height, V_H, is related to the design wind speed V by

$$V_H = C_H V, \quad (3)$$

where C_H is a correction factor for variation in the mean wind speed and gustiness with height, evaluated at height H. For the design purpose, instead of using the mean velocity as a measure of the failure velocity, it is proposed the condition for the paver failure is expressed as Eq. (4).

$$V_H = V_F \quad (4)$$

Such an approach involved a reasonable level of safety margin discussed by Bienkiewicz and Meroney[4]. Application of the described methodology using the Uniform Building Code[5] and ANSI Standard[6] is illustrated in the following sections.

5.1 Application of Uniform Building Code

The uniform Building Code recommends a coefficient, $C_e(z)$, to correct for combined height, exposure and gust factor. It can be interpolated and replaced by a smooth variation of C_e with height H as follows

$$C_e(z \le 120 \text{ ft}) = az^2 + bz + c$$

$$C_e(z > 120 \text{ ft}) = dz + e, \quad (5)$$

where z = height(ft), and a, b, c, d, e = constants. The paver failure condition expressed in Eq. (4) can be stipulated by using information on the effects of height, exposure and gustness, expressed by coefficient $C_e(H)$,

$$C_e(H) \equiv C_e(z = H) \cong C_H^2 = (\frac{V_F}{V})^2 \quad (6).$$

The maximum building height, H, can be then computed using Eqs. (5) and (6) for any exposure, design wind speed, and parapet height;

$$(H \le 120) = \frac{-b \pm \sqrt{b^2 - 4a[\ c - (\frac{V_F}{V})^2]}}{2a}$$

$$(H > 120) = \frac{1}{d}[\ (\frac{V_F}{V})^2 - e]\ . \quad (7)$$

Table 2] shows the such calculation for the uniform building code.

Table 2] Maximum Building Height Based on Experimental Data and Building Codes

	UBC			ANSI		
Basic Wind Speed [mph]	Exposure A	Exposure B	Exposure C	Exposure A	Exposure B	Exposure C
70	Not Specified	90	106	216	102	132
80		34	24	130	44	40
90				76	21	14
100				48	11	
110				32		
120				22		

5.2 Application of ANSI Standard

The pressure exposure coefficient K_z and the gust response factor G_z are defined in ANSI

$$K_z = 2.58(z/z_g)^{2/\alpha} \quad \text{for } z > 15 \text{ ft, and} \quad (8)$$

$$G_z = 0.65 + 3.65T_z \text{ , and } T_z = 2.35\, D_0^{1/2}/(z/30)^{1/\alpha}, \tag{9}$$

where z = height (ft); z_g = gradient height (ft); α = the power coefficient and D_0 = surface drag coefficient. Substitution of Eqs. (8) and (9) into Eq (4) leads to the following expression for the maximum building height;

$$H = 30\left\{\frac{-13.5(D_0)^{1/2} + \sqrt{174D_0 + 2.4(\frac{z_g}{30})^{2/\alpha}(\frac{V_F}{V})^2}}{2}\right\}^{\alpha}. \tag{10}$$

The numerical results are summarized in Table 2].

5.4 Comparison of the Results Obtained Using UBC[5] and ANSI[6]

Comparing the maximum building heights summarized in Table 2] shows that the values computed using the parameters recommended by UBC and ANSI are different, with those based on UBC recommendations being more conservative. This study confirms observations made by other researchers that failure speed is dependent on wind exposure and associated turbulence intensity, parapet height, and the presence of paver interlocks.

6. Concluding Remarks

The results of the study indicate that wind effects on and failure of ballast paver are of complicated nature suggesting more rigorous investigations are needed. However, the results of the present study are in good agreement with results of studies conducted by other researchers. Based on the presented study several observations and remarks can be made.

A. Reduction of the underneath rib height significantly reduced the wind uplift and improved the wind-resistance properties of the paver.
B. The interlock design of the paver provided the potential for the paver to withstand high wind speeds; intensive researches are necessary for the case of roof edge attached loose-laid roof paver systems.
C. The failure wind speed (the mean rooftop wind speed corresponding to paver failure) is affected by wind exposure and parapet height.
D. As the level of turbulence in the approach wind increases, the failure wind speed decreases.
E. High roof parapets increase failure wind speed, and very low roof parapets should be avoided because they reduce the failure wind speed.
F. The procedure used to determine the failure wind speed ensured conservative values for the failure wind speed.

References

1. Hee-Jung Ham, B. Bienkiewicz, and Y. Sun (1993), "Wind Tunnel Study of Hanover Paver." *Technical Report No.2-9 8680, Fluid Dynamics and Diffusion Laboratory*, Colorado State university, Fort Collins, Colorado, USA.
2. Sun, Y (1993), Wind Loading on Loose-Laid Roofing Paver Systems, Ph.D. Dissertation, Fluid Mechanics and Wind Engineering Program, Civil Engineering Department, Colorado State University, Fort Collins, Colorado, USA.
3. Hee-Jung Ham (1995), "Wind Resistant Design for Loose-Laid Roof Paver System", To be submitted, *EASEC-5*, Gold Coast, Queensland, Australia.
4 Bienkiewicz, B. and R.N. Meroney, (1988), "Wind Effects on Roof Ballast Pavers", *Journal of Structural Mechanics*, Proc. ASCE, USA, Vol. 114, pp. 1250-1267.
5. "Unifrom Building Code" (1988), *International Conference of Building Officials*, Whittier, California, USA.
6. "Minimum Design Loads for Buildings and Other Structures" (1990), ANSI/ASCE7-88, *American National Standards Institute, Inc.*, New York, N.Y., USA.